Finite-difference approach to edge-state transport in quantum wires and multiterminal devices

Florian Gagel and Klaus Maschke
Institut de Physique Appliquée, Ecole Polytechnique Fédérale, CH 1015 Lausanne, Switzerland
(Received 12 December 1994)

We investigate multimode electronic transport in a quantum wire in the presence of a uniform magnetic field. Using a finite-difference scheme for the evaluation of the free-electron Schrödinger equation, we obtain Harper's equation, which is transformed into an eigenvalue problem. The resulting scattering states of the wire are used to describe the magnetoconductance for free electrons as well as for a periodic lattice potential. In the latter case we obtain a conductance pattern that is related to the Hofstadter butterfly. The calculated current distribution in a disordered quantum Hall device confirms the edge-state picture of the transport in the quantum Hall regime.

I. INTRODUCTION

Electronic transport in the presence of a magnetic field exhibits many exciting phenomena that continue to attract the interest of both experimentalists and theorists.[1] The basis of the understanding of dc transport in the mesoscopic regime was provided by Landauer,[2,3] who related the conductance of a system to its scattering properties. The generalization of the Landauer-conductance formula to multiterminal systems by Büttiker[4] can easily be adapted to the different experimental situations, and has been used with great success for the study of a large variety of quantum-interference phenomena. In particular, it has lead to a profound understanding of the integer quantum Hall effect (IQHE).[5,6]

The scattering matrix for electrons near the Fermi energy E_F is the central quantity in the Landauer description of electronic dc transport. We, therefore, investigate first the scattering states of a quantum wire of finite width in the presence of a magnetic field. Each propagating mode at E_F adds $2e^2/h$ to the conductance of the wire. This result was originally derived for a one-dimensional waveguide. One might therefore wonder whether it remains true in the presence of a magnetic field. We prove its validity for an arbitrary Hamiltonian with translational invariance in the transport direction.

In order to keep our approach as flexible as possible, we use a finite-difference approach, which has already been used for the study of the transport properties of perturbed quantum wires in the absence of a magnetic field.[7] Starting from the Schrödinger equation and including the magnetic field, we obtain the well-known Harper equation.[8] Choosing a sufficiently high density of grid points, we can accurately describe the case of a two-dimensional free-electron gas (2DEG), which is usually employed for the discussion of the quantum Hall effect. Our approach can also be used to study the effects of a lattice-periodic potential. In the latter case, the dependence of the conductance on E_F and on the magnetic field is described by a fractal and self-similar diagram, which is closely related with the well-known Hofstadter butterfly.[8] This diagram may be used to study the increasing influence of the lattice for increasing magnetic field, or alternatively, to describe the effects of discretization in the numerical modeling of the 2DEG.

Recently, Skjånes, Hauge, and Schön[9] presented a similar pattern for the conductance, using a surface Green's function technique. However, while these authors assumed a magnetic field extending over only a finite region of the infinite quantum wires, we allow for a homogeneous magnetic field over the whole system up to the contact regions.

The existence of Hofstadter-like magnetotransport spectra has been established theoretically for weak superlattice potentials,[10] for lattices of crossed quantum wires,[11] as well as for quantum dot arrays.[12] For weak superlattice potentials, an experimental and theoretical discussion of magnetoresistance oscillations has been given in Ref. 13.

In Sec. II, we derive Harper's equation starting from the free-electron Hamiltonian, while this equation is usually derived directly from a tight-binding or Anderson Hamiltonian,[8] or is taken itself as starting point.[9] We show that Harper's equation can be transformed into a linear eigenvalue problem, which is very convenient for numerical calculations.

In Sec. III we apply our approach to six-terminal quantum Hall devices with and without disorder. The calculated spatial current distributions demonstrate the formation of edge states, thereby confirming the edge-state picture of the quantum Hall effect developed by Büttiker.[5]

II. ELECTRONIC TRANSPORT IN A QUANTUM WIRE

We consider a quantum wire of width L in the presence of a perpendicular magnetic field B. The wire is confined in the y direction, i.e., $0 \leq y \leq L$, and infinite in the

0163-1829/95/52(3)/2013(7)/$06.00

direction (see Fig. 1). Using the Landau gauge, we obtain for the vector potential $A_y = 0$, $A_x = -By$. In the presence of a spatial potential $v(x,y)$, the Hamiltonian reads $H = \frac{1}{2m_0}\left[(\frac{\hbar}{i}\partial_x - eA_x)^2 - \hbar^2\partial_y^2\right] + v(x,y)$. With the above choice for the vector potential we have $\partial_x A_x = -\partial_x By = 0$, which leads to

$$H = \frac{\hbar^2}{2m_0}\left(-\partial_x^2 + 2i\frac{e}{\hbar}By\partial_x + \frac{e^2}{\hbar^2}y^2B^2 - \partial_y^2\right) + v(x,y).$$

The Schrödinger equation is evaluated in a finite-difference scheme, using discrete values to represent the wave function ψ, with stepsize $a = L/(M+1)$, i.e.,

$$\psi(x,y) \to \psi(na, ma) := \psi_{n,m}.$$

Imposing hard-wall boundary conditions at the borders, we put $\psi_{n,0} = 0$ and $\psi_{n,M+1} = 0$. The Schrödinger equation becomes

$$\frac{\hbar^2}{2m_0 a^2}\Big[(4 + v_{nm})\psi_{n,m} - \psi_{n-1,m} - \psi_{n+1,m} - \psi_{n,m-1} - \psi_{n,m+1} + i\frac{e}{\hbar}Bma^2(\psi_{n+1,m} - \psi_{n-1,m}) - a^4\frac{e^2}{\hbar^2}m^2B^2\psi_{n,m}\Big] = E\psi_{n,m}.$$

In the B^2 term, we replace ψ_{nm} by the average $(\psi_{n-1,m} + \psi_{n+1,m})/2$ and use

$$1 + i\frac{e}{\hbar}ma^2B - \frac{e^2}{2\hbar^2}m^2a^4B^2 \approx \exp\left(2\pi i m\frac{e}{h}Ba^2\right), \quad (1)$$

which is correct up to second order in ma^2. In the exponential we recognize the ratio of the flux through one grid cell, Ba^2, and the flux quantum h/e. Following the notation of Ref. 8, we denote this ratio by

$$\alpha = \frac{e}{h}Ba^2. \quad (2)$$

With the energy scale

$$\epsilon = 2m_0 E a^2/\hbar^2, \quad (3)$$

we obtain

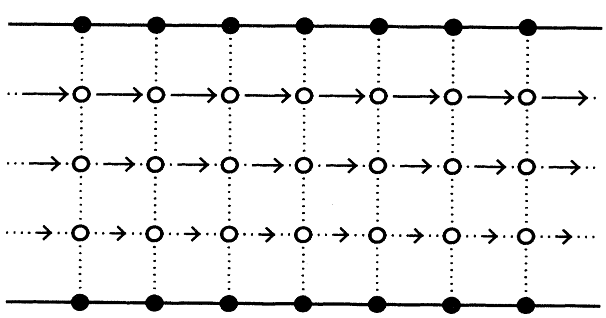

FIG. 1. A discretized quantum wire. The arrows show the local vector potential in the Landau gauge.

$$(4 + v_{nm})\psi_{n,m} - \psi_{n-1,m}e^{2\pi i m\alpha} - \psi_{n+1,m}e^{-2\pi i m\alpha} - \psi_{n,m-1} - \psi_{n,m+1} = \epsilon\,\psi_{n,m}. \quad (4)$$

In the following, we first consider perfect quantum wires, which correspond to $v_{nm} = w_m$. The Hamiltonian then becomes invariant with respect to translations in the x direction. According to the Bloch-Floquet theorem, we can therefore write the solutions as

$$\psi_{n,m} = \kappa^n\varphi_m.$$

The factor κ accounts for the spatial translation along the direction of the quantum wire. For $|\kappa| = 1$ we have propagating modes. In this case κ can be expressed in terms of the Bloch wave vector k as $\kappa = \exp(i\,ka)$.

Introducing $\tilde{\epsilon} = 4 - \epsilon$, we obtain Harper's equation

$$\varphi_m\,(\tilde{\epsilon} + w_m - e^{2\pi i m\alpha}\kappa^{-1} - e^{-2\pi i m\alpha}\kappa) - \varphi_{m-1} - \varphi_{m+1} = 0, \quad m = 1,\ldots,M. \quad (5)$$

In Appendix A we show that this system of equations can be transformed into a linear eigenvalue problem, yielding the unknowns κ and ϕ_j. From the complex conjugate system of equations, it follows immediately that, if κ is a solution, then $(\kappa^*)^{-1}$ is also a solution. The two solutions coincide for $|\kappa| = 1$. Only propagating modes with $|\kappa| = 1$ contribute to the conductance of the infinite wire. They may be distinguished by the direction of the corresponding currents. In a perfect wire we have no backscattering, and each propagating mode at the Fermi energy contributes $2e^2/h$ to the conductance. In Appendix B we show that this result, which was originally derived for 1D waveguides,[2] remains valid for any system that is translationally invariant in the direction of the propagation, and can therefore also be applied to our situation of a waveguide in a perpendicular magnetic field. The conductance G is then given by

$$G = n_c\frac{2e^2}{h}, \quad (6)$$

with n_c being half the number of *propagating* solutions $|j\rangle$ of Eq. (5) at the Fermi energy, the other half corresponding to modes that transport the current in the opposite direction.

The numerical results for $w_m = 0$ are presented in Fig. 2, where we show the calculated number of propagating channels n_c [or the conductance, see Eq. (6)] as a function of ϵ and α. Apparently, the pattern for the conductance follows closely the structure of the Hofstadter butterfly.[8] There is, however, an important difference, which can be attributed to the different choice of boundary conditions: As already pointed out in Ref. 9, Hofstadter considers the case of an infinite lattice in a magnetic field with *open* boundaries, which is also infinite in the y direction. He assumes periodicity of the eigenfunctions in the index m, with *all* possible integer periods. This leads to solutions for *rational* values of the flux α. Therefore, the structures in the Hofstadter butterfly consist of isolated points that correspond to extended states

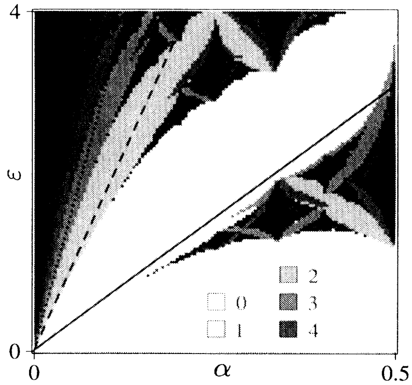

FIG. 2. Number of propagating modes contributing to the transport in one direction as a function of energy ϵ and magnetic field parameter α. The width of the wire is $M = 50$.

or propagating modes in the absence of a confining potential, while there are no solutions in the empty or white regions. Our present case is different in one important aspect: we discuss the solutions for a system that is *confined* in the y direction. The reflecting boundaries in the quantum wire lead to a different type of solutions, located in the empty regions of the Hofstadter butterfly and responsible for the conductance in the *plateau* regions (see Fig. 2). These new modes can therefore be identified as "edge states." The edge-state character of the wave functions contributing to the plateaus in the conductance becomes also evident, when looking at their spatial extension: These states are strongly localized near either of the two boundaries $m = 0$ and $m = M$, depending on the directions of the magnetic field and the current.

The dependence of the conductance pattern in Fig. 2 on the width L of the quantum wire can be studied by changing the number of grid points M for fixed lattice constant a. At zero magnetic field, the conductance scales with L. For small magnetic fields, the number of conductance plateaus and therefore the conductance itself still increase with L. This behavior is readily explained by the respective increase of the number of available propagating modes. The situation becomes different for large magnetic fields, where the conductance becomes eventually independent of L or M. This corresponds to the fact that in the high-field regime the only surviving conducting channels are edge states, which are located at the reflecting boundaries; therefore they do not depend on the width of the quantum wire.

The separation of the conductance plateaus can be related with the Landau levels of a free-electron gas. The energetic position of the νth Landau level is

$$E_\nu \;=\; (\nu + \tfrac{1}{2})\hbar\omega_c \;=\; (\nu + \tfrac{1}{2})\,\hbar\,\frac{eB}{m_0}.$$

From Eqs. (2) and (3), we obtain for the corresponding value ϵ_ν

$$\epsilon_\nu = 4\,\pi\,(\nu + 1/2)\,\alpha.$$

The first three Landau levels are indicated in Fig. 2. It is seen that for small ϵ and α, the Landau levels separate between the different plateaus. This parameter range corresponds to the case of the free-electron gas.[14] For larger ϵ or α values, lattice scattering leads to a splitting of the Landau levels into subbands, and the conductance follows the complex pattern of the Hofstadter butterfly.

III. ELECTRONIC TRANSPORT IN A QUANTUM HALL DEVICE

The above description of the conducting modes in a single quantum wire provides the basis for the understanding of transport in a multiterminal device in the presence of a magnetic field. In the following we concentrate on the example of the six-terminal quantum Hall device shown in Fig. 3. The perpendicular magnetic field extends over the whole sample, including the contact regions. The sample is connected to six external electron reservoirs with chemical potentials $\mu_1, \ldots, \mu_6$. The corresponding leads are represented by semi-infinite perfect waveguides. They act as "filters," which prevent direct tunneling from the electron reservoirs into the sample, i.e., only propagating modes can contribute to the current. This system can be described using the Landauer-Büttiker theory, which relates the transport properties of the considered sample to its scattering properties. Denoting the transmission probabilities for electrons entering the sample by channel j and leaving the sample through channel i by T_{ij}, we obtain for the current in terminal i

$$I_i = \frac{2e}{h}\sum_j (T_{ji}\mu_i - T_{ij}\mu_j). \tag{7}$$

The voltages at terminals i and j are related with the corresponding chemical potentials μ_i and μ_j by

$$U_i - U_j \equiv U_{i,j} = -(\mu_i - \mu_j)/e. \tag{8}$$

The transmission probabilities T_{ij} are obtained from the scattering amplitudes $S_{il,jk}$ between the propagating modes k and l in the waveguides at terminals j and i, respectively, i.e., we have

$$T_{ij} = \sum_{l,k} |S_{il,jk}|^2. \tag{9}$$

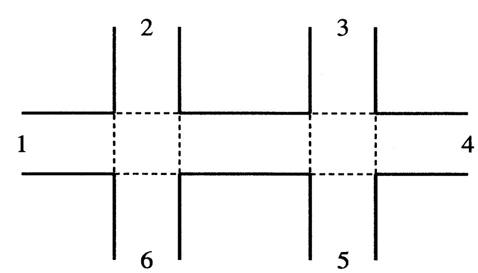

FIG. 3. A six-terminal Hall device.

For later convenience, we rewrite Eq. (7) as an Onsager equation

$$I_i = \frac{2e}{h} \sum_j \tilde{T}_{ij} \mu_j, \tag{10}$$

with $\tilde{T}_{ij} = -T_{ij}$, $j \neq i$, and $\tilde{T}_{ii} \equiv \sum_{j \neq i} T_{ji}$.

Current conservation follows from the unitarity of the scattering matrix S. In order to calculate the scattering matrix, we first solve the Schrödinger equation in the sample region for scattering boundary conditions, and then match the obtained solutions at the sample boundaries to the propagating and evanescent modes in the waveguides, which were discussed in the previous section. We use an appropriate gauge that coincides with the Landau gauge in the attached waveguides. In the following, we present the results for the situation of a Hall experiment. The current is driven by the applied voltage $U_{1,4} = -(\mu_1 - \mu_4)/e$ between contacts 1 and 4. We put $\mu_1 = \mu$ and $\mu_4 = 0$. Terminals 2, 3, 5, and 6 are used as voltage probes, i.e., we impose the current conservation conditions $I_2 = I_3 = I_5 = I_6 \equiv 0$. From the calculated scattering matrix S together with Eq. (10) we can then calculate the longitudinal resistance $R_{xx} = U_{23}/I_1$ as well as the Hall resistance $R_{xy} = U_{26}/I_1$. In Fig. 4(a) we present the results for R_{xy} and R_{xx} as a function of the magnetic field. For intermediate magnetic fields we obtain perfect quantum Hall plateaus in R_{xy} with vanishing longitudinal resistance R_{xx} in the plateau regime. The minimum magnetic field required for the formation of the plateaus depends on the width M, i.e., for larger M the plateaus are already found at smaller fields. This can be attributed to the fact, that edge states can only form when their localization length in direction across the wire becomes small compared with the width of the wire. It should be noted that Fig. 4(a) is closely related to Fig. 2, which describes the conductance of a single quantum wire. In fact, in the plateau regime, the Hall resistance R_{xy} in Fig. 4(a) corresponds precisely to the horizontal cut in Fig. 2 at the chosen Fermi energy $\epsilon = 0.5$. In other words, in the quantum Hall regime the Hall resistance R_{xy} is given by the resistance of a single quantum wire.

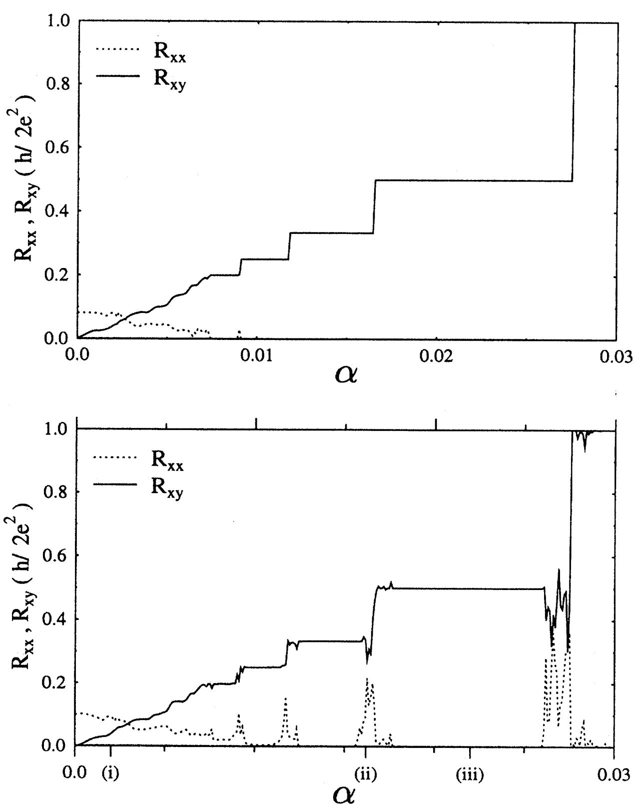

FIG. 4. Longitudinal resistance R_{xx} and Hall resistance R_{xy}. The dimensions of the sample and the width of the waveguides are given by $M = 30$, the Fermi energy is $\epsilon = 0.5$ (a) ordered sample ($W = 0$); (b) disordered sample ($W = 0.25$).

The role of disorder on the quantum Hall effect has been widely discussed in the literature.[15] In our approach, disorder can be introduced in a straightforward manner by choosing the potential values v_{nm} [see Eq. (4)] from a uniform distribution of random numbers of width $2W$, i.e., $v_{nm} \in [-W, W]$ for positions (n, m) within the sample region (dashed squares in Fig. 3). W defines the degree of disorder. The results for $W = 0.25$ are shown in Fig. 4(b), for the same parameters as in Fig. 4(a). We see that the Hall plateaus remain nearly unchanged. The influence of the disorder is, however, clearly seen in the neighborhood of the steps in the Hall resistance, where it leads to strong fluctuations of R_{xy} and R_{xx}.

The role of the edge states for the transport in the quantum Hall regime can be illustrated by the local current distributions, which are shown in Fig. 5 for the case of the disordered sample and for different magnetic fields. At small magnetic fields [see Fig. 5(a)] the current distribution is rather uniform; the slight deviations of the current are due to the presence of disorder. The situation changes completely in the quantum Hall regime. This is shown in Fig. 5(c), where we have chosen a magnetic field corresponding to a plateau in R_{xy} [see Fig. 4(b)]. Now the current distribution is strongly nonuniform, and follows closely the boundaries at one side of the sample. The disorder has practically no influence on the conductance.

Disorder becomes, however, important in the region of the steps between the plateaus. This is demonstrated in Fig. 5(b). In this region the current distribution is rather complicated: Backscattering by the impurities and by the boundaries leads to vortexlike local currents and induces coupling between the propagating modes or edge states, which are close in energy. We note, that the fluctuations of the Hall conductance are of the order of $2e^2/h$, which is also the order of the universal conductance fluctuations in disordered quantum wires.

The above results are in full agreement with Büttiker's edge-state picture.[5] According to Eq. (7), currents and potentials are described in terms of the total transmission probabilities between the contacts $T_{i,j}$. The latter may be expressed in terms of the transmission probabilities $|S_{il,jk}|^2$ for the conducting modes l and k in quantum wires i and j [Eq. (9)]. The plateau regimes are characterized by the absence of backscattering in the propagating modes [see Fig. 5(b)], and therefore we have $|S_{il,jk}|^2 = 1$ for the n_c modes in the quantum wires, which contribute to the current in forward direction. Thus, Eq. (9) yields $T_{ij} = n_c$ in the plateau regime for waveguides i and j ordered in the direction of propagation of the conducting modes, and $T_{ij} = 0$ between all other pairs of waveguides. For example, the situation of Fig. 5(b) corresponds to $T_{61} = T_{56} = T_{45} = T_{34} = T_{23} = T_{12} = n_c$, and all other transmission probabilities equal to zero. With $\mu_1 = \mu$, $\mu_4 = 0$, and imposing the current conservation conditions $I_2 = I_3 = I_5 = I_6 = 0$, we obtain from Eq. (10) $\mu_2, \mu_3 = 0$, $\mu_5, \mu_6 = \mu$, and $I_1 = (2en_c/h)\mu = -I_4$. This corresponds to the well-known results for the IQHE:

$$R_{xy} = \frac{\mu_6 - \mu_2}{eI_1} = \frac{h}{2e^2 n_c}$$

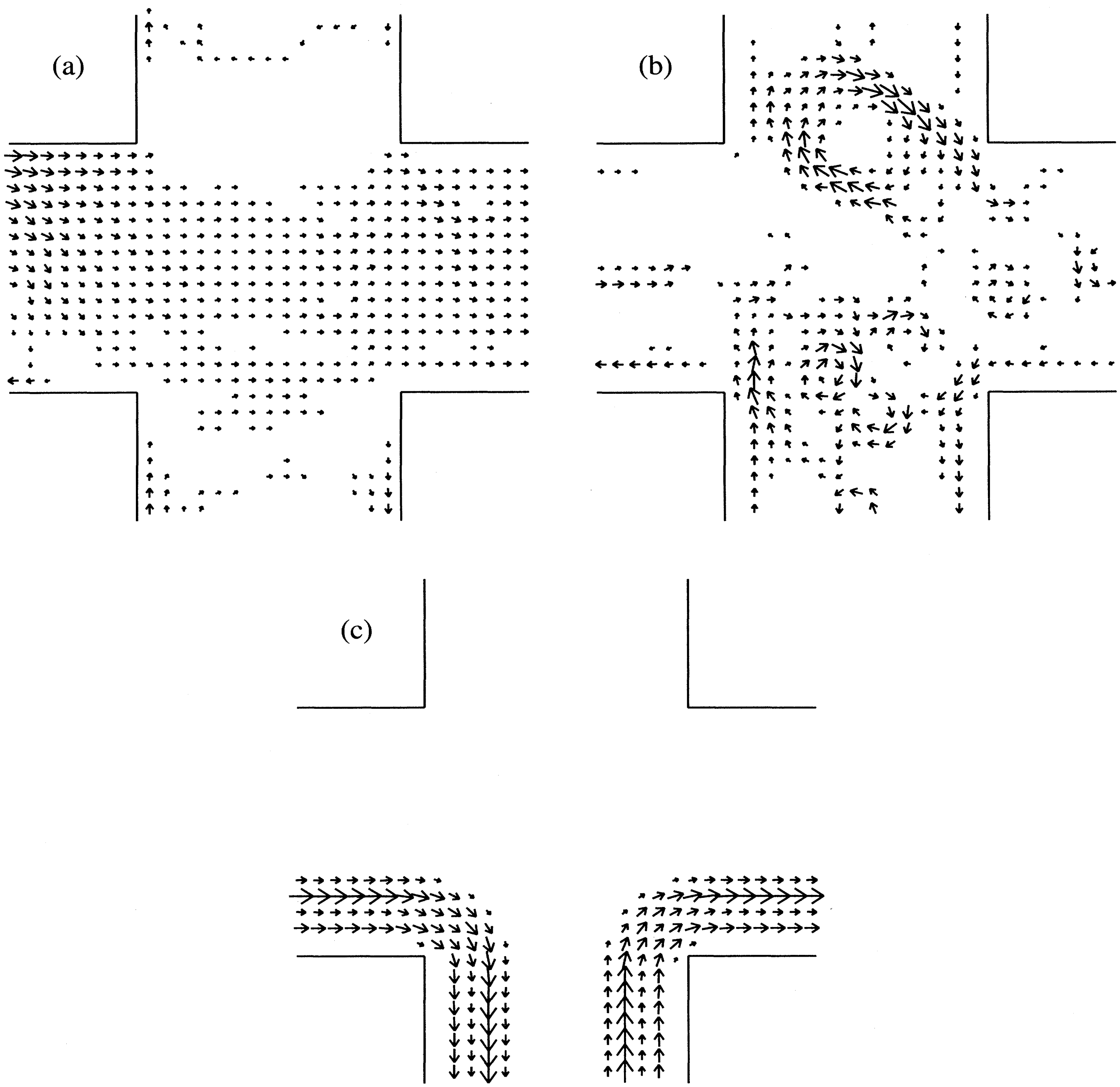

FIG. 5. Local current distributions in the disordered Hall device for different magnetic fields. The disorder parameter is the same as in Fig. 4(b) ($W = 0.25$). (a), (b), and (c) correspond to the magnetic fluxes (i), (ii), and (iii) indicated in Fig. 4(b).

and

$$R_{xx} = \frac{\mu_2 - \mu_3}{eI_1} = 0.$$

IV. CONCLUSIONS

We have presented an efficient finite-difference scheme that allows us to calculate the transport properties of two-dimensional quantum wires and multiterminal devices in a homogeneous magnetic field. The required solution of Harper's equation has been reformulated as an eigenvalue problem, thus avoiding the approximations proposed in the literature. Our results for a single quantum wire show that the present approach does not only give an excellent description of the conductance of a confined free-electron gas in a magnetic field, but that it allows also us to study the influence of backscattering in a wire with periodic lattice structure. The importance of the boundary conditions leading to edge states has been revealed by comparing the obtained conductance pattern with the Hofstadter butterfly, which describes the eigenvalue spectrum of an *infinite* lattice without borders in the presence of a perpendicular magnetic field. Using our results for a single quantum wire, we have also calculated the electronic transport in a six-terminal quantum Hall device, where we have demonstrated the stability of the quantum Hall plateaus against disorder. The results are in full agreement with the edge-state picture for the IQHE of Büttiker.[5]

ACKNOWLEDGMENT

This work was supported by the Swiss National Science Foundation under Grant No. 21-39114.93.

APPENDIX A: SOLUTION OF HARPER'S EQUATION

Defining $\gamma \equiv \exp(2\pi i\alpha)$, we write Eq. (5) as

$$\begin{aligned}\kappa\varphi_m = & -\kappa^{-1}\gamma^{2m}\varphi_m + (\tilde{\epsilon} + w_m)\,\gamma^m\varphi_m \\ & -\gamma^m\varphi_{m-1} - \gamma^m\varphi_{m+1},\end{aligned}$$

where $m = 0, \ldots, M$.

While it is an easy task to calculate the band structure of the propagating modes $\tilde{\epsilon}(k)$ for given k [or given $\kappa \equiv \exp(i\ ka)$], it is not so obvious to solve the inverse problem, i.e., to find the values of k corresponding to propagating modes for a given energy $\tilde{\epsilon}$. This is, however, the basic question to answer, since the number of transport channels is determined by the number of available k values at the given Fermi energy. Recently, an expansion method has been proposed for the continuum case.[16] Using a finite-element approach, Leng and Lent[17] have found the solutions in terms of a *nonlinear* eigenvalue problem. In the following we show that in the finite-difference approach this problem can be solved in a straightforward manner, which is numerically efficient and may also have theoretical applications. The simple trick consists in introducing M new variables

$$\lambda_m := -\kappa^{-1}\gamma^m\varphi_m. \tag{A1}$$

This leads to the new system of equations

$$\begin{aligned}\kappa\varphi_m &= \gamma^m\lambda_m + (\tilde{\epsilon} + w_m)\,\gamma^m\varphi_m - \gamma^m\varphi_{m-1} - \gamma^m\varphi_{m+1}, \\ \kappa\lambda_m &= -\gamma^m\varphi_m,\end{aligned}$$

which can be written as an eigenvalue problem $\mathbf{A}\vec{x} = \kappa\vec{x}$, with $\vec{x} = (\varphi_1, \ldots, \varphi_M, \lambda_1, \ldots, \lambda_M)^T$, and $\mathbf{A} = \begin{pmatrix} \mathbf{T} & \mathbf{D} \\ -\mathbf{D} & \mathbf{0}\end{pmatrix}$, where

$$\mathbf{T} = \begin{pmatrix} (\tilde{\epsilon}+w_1)\,\gamma & -\gamma & 0 & 0 & \cdots & 0 \\ -\gamma^2 & (\tilde{\epsilon}+w_2)\,\gamma^2 & -\gamma^2 & 0 & \cdots & 0 \\ 0 & -\gamma^3 & (\tilde{\epsilon}+w_3)\,\gamma^3 & -\gamma^3 & \ddots & 0 \\ \vdots & & \ddots & \ddots & \ddots & \vdots \\ 0 & \cdots & 0 & -\gamma^{M-1} & (\tilde{\epsilon}+w_{M-1})\,\gamma^{M-1} & -\gamma^{M-1} \\ 0 & \cdots & 0 & 0 & -\gamma^M & (\tilde{\epsilon}+w_M)\,\gamma^M \end{pmatrix}.$$

$\mathbf{D} = (d_{ij})$, $d_{ij} = \delta_{ij}\gamma^i$, and $\mathbf{0}$ is the $M \times M$ null matrix. We note that this eigenvalue problem is equivalent to the generalized eigenvalue problem of Ref. 18.

The wave functions corresponding to the $2M$ eigenvalues κ_j are given by the first M components of the eigenvectors. The second half of the eigenvectors contains the $\lambda's$, which fulfill Eq. (A1); this may be verified after the numerical solution for testing purposes. From the numerical point of view, this method has proven to be stable and can easily cope with system sizes M larger than 100.

APPENDIX B: CONDUCTANCE FOR TRANSLATION-INVARIANT SYSTEMS

We consider a translation-invariant wire connected at both ends to electron reservoirs with chemical potentials μ_1 and μ_2. The corresponding voltage difference is $\mu_1 - \mu_2 = -eU$. The translational invariance of the system implies that in our Landau gauge the Hamiltonian commutes with the translation operator in x direction, i.e., the eigenfunctions of the Hamiltonian are given by Bloch waves $\mid \nu, k\,\rangle$.

The current is given by

$$I_{\text{tot}} = \sum_\nu I_\nu \left.\frac{\partial n_\nu}{\partial E}\right|_{E=E_F} (\mu_1 - \mu_2)$$
$$= \sum_\nu I_\nu \frac{\partial n_\nu}{\partial k} \left.\frac{\partial k}{\partial E}\right|_{E=E_F;k=k_\nu} (\mu_1 - \mu_2). \quad \text{(B1)}$$

I_ν is the current of a propagating mode ν at E_F, normalized over a given normalization length, $\partial n_\nu/\partial E$ is the respective density of states. Taking the spin degeneracy into account, we obtain for the one-dimensional k space density per normalization length $\partial n_\nu/\partial k = 1/\pi$.

The current-density operator can be expressed by the commutator of the Hamiltonian with the position operator $\hat{x}$:

$$\hat{j} = e\partial_t\, \hat{x} = e\frac{i}{\hbar}[\hat{H},\, \hat{x}].$$

We choose the k representation and obtain for the expectation value of the current in x direction

$$I_\nu = \left\langle \nu, k \,\middle|\, i\,\frac{e}{\hbar}[\hat{H},\, -i\partial_k] \,\middle|\, \nu, k \right\rangle$$
$$= \frac{e}{\hbar}\langle\, \nu, k \mid E(k)\partial_k \, - \partial_k\, E(k) | \, \nu, k \,\rangle$$
$$= -\frac{e}{\hbar}\langle\, \nu, k \mid \nu, k \,\rangle\, \frac{\partial E}{\partial k},$$

i.e.,

$$\frac{\partial k}{\partial E}\, \frac{I_\nu}{\langle \nu, k|\nu, k\rangle} = -\, e/\hbar.$$

Inserting this in Eq. (B1) and using Eq. (8), we obtain

$$I_{\text{tot}} = n_c\, \frac{2e^2}{h}\, U,$$

where n_c is the number of propagating states at E_F.

[1] For an overview, see, e.g., C.W.J. Beenakker and H. van Houten, in *Solid State Physics: Advances in Research and Applications*, edited by H. Ehrenreich and D. Turnbull (Academic, New York, 1991), Vol. 44, and references therein

[2] R. Landauer, IBM J. Res. Dev. **1**, 223 (1957); Philos. Mag. **21**, 863 (1970).

[3] R. Landauer, Z. Phys. B **68**, 217 (1987); J. Phys. Condens. Matter **1**, 8099 (1989).

[4] M. Büttiker, Phys. Rev. Lett. **57**, 1761 (1986).

[5] M. Büttiker, Phys. Rev. B **38**, 9375 (1988).

[6] A.M. Chang, in *Electronic Structure and Properties of Semiconductors*, edited by W. Schroeter (VCH, Weinheim, 1991), p. 449.

[7] C. Berthod, F. Gagel, and K. Maschke, Phys. Rev. B **50**, 18 299 (1994).

[8] D.R. Hofstadter, Phys. Rev. B **14**, 2239 (1976).

[9] J. Skjånes, E.H. Hauge, and S. Schön, Phys. Rev. B **50**, 8636 (1994).

[10] S. Ishizaka, K. Nakamura, and T. Ando, Phys. Rev. B **48**, 12 053 (1993).

[11] F. Gagel and K. Maschke, Phys. Rev. B **49**, 17 170 (1994).

[12] G. Kirczenow, Surf. Sci. **263**, 330 (1992).

[13] R. R. Gerhardts, D. Weiss, and U. Wulf, Phys. Rev. B **43**, 5192 (1991).

[14] Using our energy scaling, Eq. (3), one obtains for the Fermi energy $\epsilon = 2\pi\, a^2\, n$, where n is the electron density of the 2DEG. Taking $n = 4 \times 10^{15}$ m^{-2} and a quantum wire of width $L = 100$ nm, $M = 20$ gridpoints would hence be needed in order to arrive at $\epsilon < 1$, which is needed for an adequate description of the free-electron parabola by the sinusoïdal dispersion corresponding to the Anderson Hamiltonian. For the respective value of $a = 5$ nm, a magnetic field of $B = 1$ T corresponds to $\alpha = 0.006$. Equation (1) is thus an excellent approximation for all experimentally accessible values of B.

[15] See, e.g., K. Shepard, Phys. Rev. B **44**, 9088 (1991).

[16] Zhen-Li Ji, Phys. Rev. B **50**, 4658 (1994).

[17] M. Leng and C.S. Lent, J. Appl. Phys. **76**, 2240 (1994).

[18] A. MacKinnon, Z. Phys. B **59**, 385 (1985).

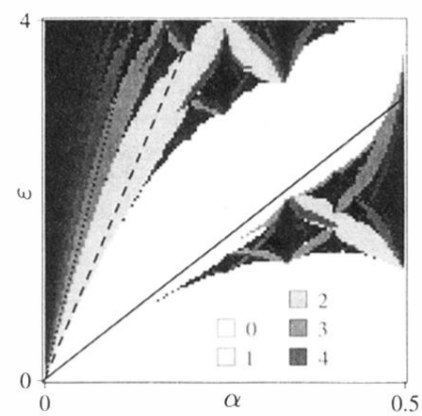

FIG. 2. Number of propagating modes contributing to the transport in one direction as a function of energy ϵ and magnetic field parameter α. The width of the wire is $M = 50$.